

Effect of Infiltration  
Ce<sub>0.8</sub>Sm<sub>0.2</sub>O<sub>1.9</sub> Against  
Double Perovskite Performance  
LaBa<sub>0.5</sub>Sr<sub>0.5</sub>Co<sub>2</sub>O<sub>5+δ</sub> as IT-  
SOFC Cathode

*by* Subardi -

---

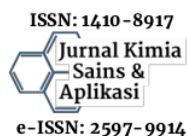
**Submission date:** 23-Mar-2023 06:37PM (UTC-0700)

**Submission ID:** 2044962862

**File name:** 48173-164961-1-PB.pdf (722.53K)

**Word count:** 4038

**Character count:** 22167



## Effect of Infiltration $\text{Ce}_{0.8}\text{Sm}_{0.2}\text{O}_{1.9}$ Against Double Perovskite Performance $\text{LaBa}_{0.5}\text{Sr}_{0.5}\text{Co}_2\text{O}_{5+\delta}$ as IT-SOFC Cathode

Adi Subardi <sup>a,\*</sup>, Yen-Pei Fu <sup>b</sup><sup>a</sup> Department of Mechanical Engineering, Yogyakarta National Institute of Technology (ITNY), Yogyakarta 55281, Indonesia<sup>b</sup> Department of Materials Science and Engineering, National Dong Hwa University, Hualien 97401, Taiwan\* Corresponding author: [subardi@itny.ac.id](mailto:subardi@itny.ac.id)<https://doi.org/10.14710/jksa.25.10.346-351>

### Article Info

#### Article history:

Received: 9<sup>th</sup> August 2022Revised: 20<sup>th</sup> November 2022Accepted: 13<sup>th</sup> December 2022Online: 25<sup>th</sup> December 2022

#### Keywords:

IT-SOFC; Cathode; Infiltration;  
Electrochemical properties;  
Symmetrical cell

### Abstract

Modifying the sample surface by infiltration technique using  $\text{Ce}_{0.8}\text{Sm}_{0.2}\text{O}_{1.9}$  (SDC) electrolyte has been done to increase the catalytic activity of the  $\text{LaBa}_{0.5}\text{Sr}_{0.5}\text{Co}_2\text{O}_{5+\delta}$  (LBSC) cathode. The cathode powder structure was evaluated using X-ray diffraction (XRD) at room temperature, and the LBSC cathode microstructure was analyzed using scanning electron microscopy (SEM). The electrical conductivity of the LBSC cathode was tested using the four-probe DC method. Symmetrical cells were tested using a potentiostat Voltalab PGZ 301 and a digital source meter Keithley 2420. LBSC powder was discovered to have a tetragonal structure (space group:  $P4/mmm$ ) with lattice parameters of  $a = 3.86253 \text{ \AA}$ ,  $c = 7.73438 \text{ \AA}$ , and  $V = 115.338 \text{ \AA}^3$ . From the SEM image, the LBSC cathode has homogeneous, dense, and highly porous grains. The electrical conductivity showed metallic behavior, gradually decreasing from  $167 \text{ S}\cdot\text{cm}^{-1}$  at  $300^\circ\text{C}$  to  $105 \text{ S}\cdot\text{cm}^{-1}$  at  $800^\circ\text{C}$ . A significant increase in current density ( $i_0$ ) of 275% occurred at  $800^\circ\text{C}$  from  $154.10 \text{ mA}\cdot\text{cm}^{-2}$  (pure LBSC) to  $577.86 \text{ mA}\cdot\text{cm}^{-2}$  (LBSC+0.5M SDC). The activation energy value ( $E_a$ ) of symmetrical cells was determined using electrochemical impedance spectroscopy (EIS), low-field (LF), and high-field (HF) techniques. The activation energy of the LBSC+0.5 M SDC specimen was  $47.9 \text{ kJ mol}^{-1}$  or 79.4% lower than the activation energy of the LBSC cathode specimen without infiltration at atmospheric pressure of 0.03 atm. These results indicate that SDC infiltration of the LBSC cathode can reduce the activation energy of the significant. The cathode membrane adheres quite well to the electrolyte membrane, the cathode porosity varies in the range of 1–4  $\mu\text{m}$ , and the grain size is 0.1–1.5  $\mu\text{m}$ .

### 1. Introduction

Intermediate temperature solid oxide fuel cell (IT-SOFC) has the advantage of being one of the most eco-friendly energies and performs a direct transformation of fuel into electrical energy [1]. High working temperatures limit the application of SOFC due to the potential degradation of SOFC components and costly operations. Moreover, the lower SOFC operating temperature causes slower oxygen reduction kinetics, and a high over-potential occurs at the cathode and dramatically reduces the electrochemical activity of the cathode [2, 3].

Lowering the operating temperature allows SOFCs to overcome several challenges, such as reducing thermal degradation, enabling the utilization of inexpensive metal interconnection materials, and suppressing reactions between cell components, all of which lower operational costs for SOFCs. Generally, the cathode becomes the limiting factor for determining the overall cell performance. Therefore, novel SOFC electrodes with high electrocatalytic activity must be developed [4, 5]. Perovskite and its structural variants are utilized as high-performance cathodes for IT-SOFC. Cobaltite which has excellent electrochemical properties,

has been studied as a cathode material for IT-SOFCs [6, 7].

Double perovskites are suitable as IT-SOFC cathode materials, which require greater surface exchange kinetics and faster oxygen diffusion rates in a moderate temperature range [8]. Oxygen can migrate rapidly across the LnO field on perovskite sites with the order  $\text{LnBaCo}_2\text{O}_{5+\delta}$ , as evaluated by neutron diffraction [9].  $\text{LaBa}_{0.5}\text{Sr}_{0.5}\text{Co}_2\text{O}_{5+\delta}$  (LBSC) double perovskite was selected as the cathode material in this study. This study aimed to investigate infiltration techniques to enhance SOFC performance even though LBSC characterization, such as crystal structure, weight loss, thermal expansion characteristics, microstructure, and electrochemical properties, has already been examined. Due to the relatively high activation energy required for the oxygen reduction reaction, the electrochemical resistance of SOFC components, particularly the cathode, will increase with decreasing operating temperature (ORR) [10]. Therefore, many researchers make great efforts to reduce the cathode's polarization resistance ( $R_p$ ) to improve the cathode's performance [11, 12]. One of the practical and cost-effective approaches for cathode surface modification through wet chemical infiltration can increase catalytic activity [13].

Based on the literatures [14, 15, 16, 17, 18, 19], there was a significant decrease in cathode polarization resistance after infiltration. For example, the area-specific resistance (ASR) or  $R_p$  values of the cathode  $\text{La}_{0.6}\text{Sr}_{0.4}\text{Co}_{0.2}\text{Fe}_{0.8}\text{O}_{3-\delta}$  (LSCF) were  $0.4 \Omega\cdot\text{cm}^2$ ,  $0.15 \Omega\cdot\text{cm}^2$ , and  $0.064 \Omega\cdot\text{cm}^2$  at  $700^\circ\text{C}$ ,  $750^\circ\text{C}$ , and  $800^\circ\text{C}$ , after infiltrating  $0.25 \text{ mol L}^{-1}$   $\text{Ce}_{0.8}\text{Sm}_{0.2}\text{O}_{1.9}$  (SDC) into the porous LSCF, the  $R_p$  values decreased to  $0.17 \Omega\cdot\text{cm}^2$ ,  $0.074 \Omega\cdot\text{cm}^2$ , and  $0.041 \Omega\cdot\text{cm}^2$  at  $700^\circ\text{C}$ ,  $750^\circ\text{C}$ , and  $800^\circ\text{C}$ . The LCF electrode experienced a significant decrease in  $R_p$  value after being infiltrated with SDC, indicating an increase in electrochemical activity [20].

The  $R_p$  value of the cathode  $\text{SmBa}_{0.5}\text{Sr}_{0.5}\text{Co}_2\text{O}_{5+\delta}$  (SBSC55) decreased from  $4.17 \text{ cm}^2$  at  $600^\circ\text{C}$  to  $0.35 \text{ cm}^2$  at  $800^\circ\text{C}$ , as previously reported by Subardi and Fu [21]. The  $R_p$  value was significantly reduced when the SDC nano electrolyte was infiltrated into the pure SBSC55 cathode, indicating the presence of both electrochemical processes. This electrochemical process, specifically the electrochemical reaction between the electrode-electrolyte layers and the adsorption-desorption of oxygen diffusion between the cathode-gas surface layers, was enhanced simultaneously by active SDC nanosized particles. The  $R_p$  value of porous SBSC55 decreased from  $3.82 \Omega\cdot\text{cm}^2$  at  $600^\circ\text{C}$  to  $0.24 \Omega\cdot\text{cm}^2$  at  $800^\circ\text{C}$  when  $0.13 \text{ M}$  SDC was infiltrated onto its surface.  $R_p$  values decreased to  $1.28 \Omega\cdot\text{cm}^2$ ,  $0.32 \Omega\cdot\text{cm}^2$ , and  $0.11 \Omega\cdot\text{cm}^2$  at  $600^\circ\text{C}$ ,  $700^\circ\text{C}$ , and  $800^\circ\text{C}$ , respectively, when the number of SDC doses was increased to  $0.65 \text{ M}$ . Infiltration of SDC into the  $\text{SmBa}_{0.5}\text{Sr}_{0.5}\text{Co}_2\text{O}_{5+\delta}$  cathode, as reported previously by our team, revealed SDC grains measuring between 10 and 35 nm. On the surface of the porous cathode, SDC granules are evenly and uniformly distributed, resulting in improved interconnection and electrochemical properties.

In this research paper, SDC nanoparticles were successfully infiltrated into the porous LBSC cathode to improve the electrochemical properties of the cathode. The structure and conductivity of the LBSC cathode were also investigated.

## 2. Experimental

### 2.1. Materials and Equipment

Stoichiometric amounts of  $\text{La}_2\text{O}_3$  (99%, Wako Pure Chemical Industries, Ltd.),  $\text{SrCO}_3$  (98%, Shimakyu Chemical Co., Ltd),  $\text{BaCO}_3$  (98.8%, Showa Chemical Industries, Ltd.), and  $\text{CoO}$  (99.9%, Choneye Pure Chemical Co., Ltd.) powder were used as raw materials. LBSC cathode powders were prepared using a solid-state reaction method. Detailed procedures regarding cathode fabrication can be seen in reference [22].  $\text{Ce}_{0.8}\text{Sm}_{0.2}\text{O}_{1.9}$  (SDC) powder was synthesized by coprecipitation method using  $\text{Ce}(\text{NO}_3)_3\cdot 6\text{H}_2\text{O}$  (99%, Wako Pure Chemical Industries, Ltd.) and  $\text{Sm}(\text{NO}_3)_3\cdot 6\text{H}_2\text{O}$  (99%, Wako Pure Chemical Industries, Ltd.) as starting materials. Detailed procedures regarding SDC electrolyte fabrication can refer to reference [23].

The tools were glassware, digital scales, alumina grinding balls, magnetic stirrer, digital scales, furnaces, screen printing, injectors, and vacuum tubes. The instruments used were a press machine, XRD Rigaku D/MAX-2500V, a digital source meter (Keithley 2420), VoltaLab PGZ 30 potentiostat, and Z-view.

### 2.2. Specimen Fabrication

LBSC|SDC|LBSC symmetrical cells infiltrated with SDC electrolyte by screen printing technique. LBSC double perovskite cathode paste was smeared on both sides of an SDC electrolytic disc with a diameter of 1.3 cm and a thickness of 0.1 cm. After the cathode was printed on the SDC electrolyte, the sample was sintered at  $1000^\circ\text{C}$  for 4 hours. A detailed explanation of the fabrication of symmetrical cell samples can be seen in the previous paper [21]. The symmetric cell test was tested at a furnace temperature of  $600\text{--}800^\circ\text{C}$  at  $50^\circ\text{C}$  intervals under atmospheric pressure ( $\text{O}_2$ ) of 0.21 atm.

### 2.3. Characterization and Measurement

Cathode powder  $\text{LaBa}_{0.5}\text{Sr}_{0.5}\text{Co}_2\text{O}_{5+\delta}$  (LBSC) was characterized using XRD with  $\text{Cu K}\alpha$  radiation ( $1.5418 \text{ \AA}$ ), the scanning rate of  $4^\circ/\text{min}$  and scanning range of  $20^\circ\text{--}80^\circ$ . Electrical conductivity measurement data was recorded with a digital source meter (Keithley 2420). The microstructure of the LBSC cathode was observed with a scanning electron microscope (SEM; Hitachi 3500H). AC impedance was measured using a VoltaLab PGZ 30 potentiostat. EIS (electrochemical impedance spectroscopy) was performed under cathodically polarized conditions as a function of the cathodic voltage. Z-view software was used to conduct an EIS fitting analysis.

## 3. Results and Discussion

The X-ray diffraction pattern of calcined LBSC cathode powder at  $1100^\circ\text{C}$  for 5 hours is shown in Figure 1. XRD pattern of LBSC as a double perovskite structure

without peaks due to impurities [24]. This result indicates that the LBSC cathode powder fabrication was successful. The results of the diffraction pattern fitting are in line with the ICSD 98-009-0492 database. General Structure Analysis Software (GSAS) was employed for Rietveld refinement. Based on the refinement data, it is known that the diffraction pattern of the LBSC sample has a tetragonal structure (space group:  $P4/mmm$ ) with lattice parameters  $a = 3.86253 \text{ \AA}$ ,  $c = 7.73421 \text{ \AA}$ , and  $V = 115.338 \text{ \AA}^3$ . The shift of the highest peak (102) towards the lower angle indicates the expansion of the unit cell volume.

The electrical conductivity of the LBSC cathode samples is shown in Figure 2 for the temperature range of 300–800°C and  $p(O_2)$  of 0.03 and 0.0032 atm. The conductivity significantly decreased with increasing temperature on  $p(O_2)$  of 0.03 atm, indicating metallic properties.

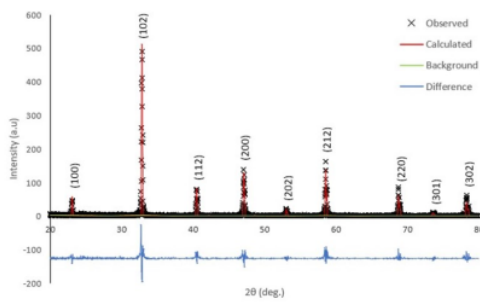


**Figure 1.** X-ray diffraction pattern of sintered LBSC cathode powder at 1100°C and Rietveld analysis using the General Structure Analysis System (GSAS) application

The reduction in conductivity occurred since the initial heating at 300°C, as shown in Figure 2. This reduction occurred due to the lattice defects of the Co–O–Co bonds, resulting in the removal of oxygen atoms from the lattice and the reduction of  $Co^{4+}$  to  $Co^{3+}$  or  $Co^{3+}$  to  $Co^{2+}$ . The LBSC cathode conductivity value ranged between 100–165  $S \cdot cm^{-1}$  and met the requirements of a SOFC cathode material [25].

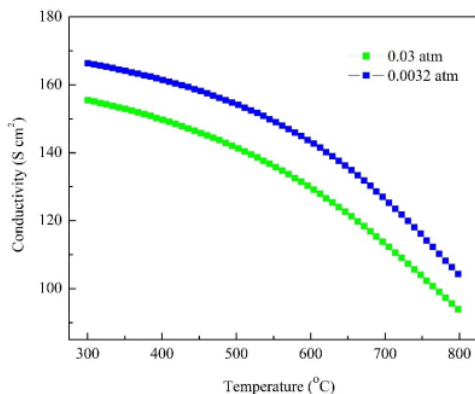


**Figure 2.** LBSC cathode conductivity at  $p(O_2)$  of 0.03 and 0.0032 atm

The energy band overlap between Co-3d and O-2p, the presence of  $Co^{4+}$  ions from the thermally generated  $Co^{3+}$  charge disproportionation, and the loss of oxygen from the lattice at higher temperatures all affect the metallic conductivity of LBSC materials [26, 27, 28]. The electrical conductivity decreased with decreasing  $p(O_2)$  at  $p(O_2)$  of 0.0032 atm ( $O_2$ ), and the trend was similar to testing under atmospheric pressure  $p(O_2)$  of 0.03 atm. Figures 3(a) and 3(b) show Nyquist plots for impedance spectroscopy of LBSC and LBSC+0.5 M SDC cathodes. As has been reported by previous studies [21], SDC infiltration towards the  $SrBa_{0.5}Sr_{0.5}Co_{2}O_{5-\delta}$  cathode revealed SDC grains in the range of 10–35 nm. SDC granules are homogeneously distributed on the surface of the porous cathode resulting in good interconnection and improved electrochemical properties. According to this circumstance, SDC nanoparticles actively promote both simultaneous adsorption-desorption of oxygen diffusion between layers of cathode-gas surface and electrochemical reactions between layers of electrode and electrolyte [21].

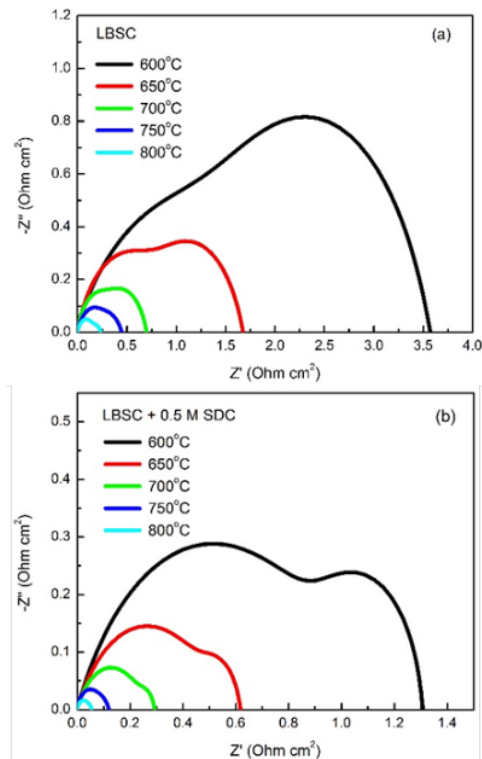


**Figure 3.** Nyquist plots for impedance spectroscopy: (a) LBSC cathode without infiltration, (b) LBSC+0.5M SDC cathode at 600–800°C

The current density parameter can be used to assess the intrinsic oxygen reduction rate and the cathode's electrochemical characteristics [29]. In this paper, a technique of electrochemical impedance spectroscopy (EIS), low-field (LF), and high-field (HF) was used to determine the value of the current density, a more detailed explanation of these three techniques can be

seen in reference [22]. The overall activation energy ( $E_a$ ) for the oxygen reduction reaction (ORR) was calculated by the Arrhenius equation (1) based on the slope of the Arrhenius plot.

$$\ln i_o = \ln K - \frac{E_a}{RT} \quad (1)$$

where  $K$  is the pre-exponential constant, determined from the y-intercept, and  $E_a$  is the activation energy of the reaction. The  $E_a$  for ORR relates to the different preparation techniques, cathode compositions, and cathode structures.

Figure 4 shows the Arrhenius plots for the current density values collected from LBSC double perovskite specimens at working temperatures between 600–800°C. The activation energy ( $E_a$ ) values of symmetrical cells were 138.0 kJ mol<sup>-1</sup>, 74.8 kJ mol<sup>-1</sup>, and 77.7 kJ mol<sup>-1</sup>, respectively, for EIS, LF, and HF, as shown in Figure 4(a).

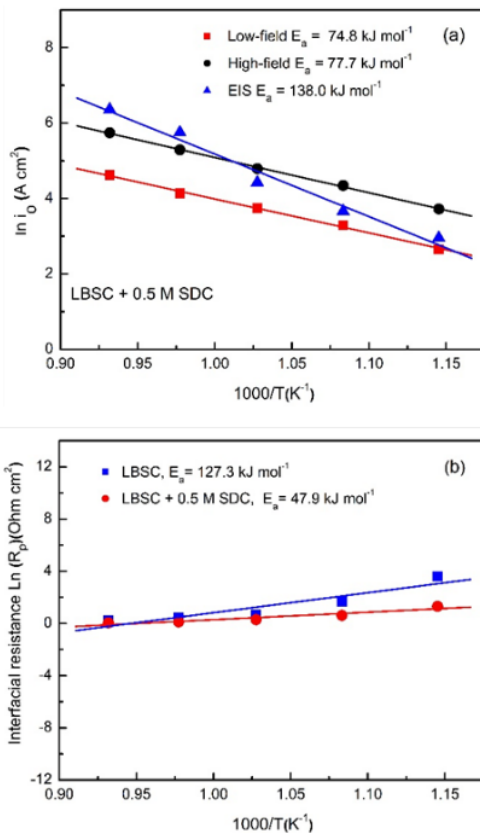


**Figure 4.** (a) Arrhenius plot for ORR of LBSC cathode on the SDC electrolyte, the obtained current density ( $i_o$ ) through the EIS, LF, and HF techniques, (b)  $\ln(R_p)$  vs.  $1000/T$  over a temperature range of 600–800°C

The linearity of the Arrhenius plot indicates that the LBSC double perovskite oxides are stable concerning temperature. The activation energy ( $E_a$ ) of the polarization resistance of LBSC+0.5 M SDC cathode from the plot  $\ln(R_p)$  vs.  $1000/T$  was 47.9 kJ mol<sup>-1</sup> or significantly decreased compared to pure specimen

[LBSC], which was 127.3 kJ mol<sup>-1</sup> or decreased by 79.4% at an atmospheric pressure of 0.03 atm as shown in Figure 4(b).

The current density of the LBSC cathode increased from 11.13 Ω.cm<sup>2</sup> at 600°C to 154.1 Ω.cm<sup>2</sup> at 800°C. The current density of the LBSC cathode increased from 3.60 to 19.19 mA.cm<sup>-2</sup> at 600°C after infiltration with 0.5 M SDC. The current density value experienced a continuous increase at 700°C from 72.28 (pure LBSC) to 83.84 mA.cm<sup>-2</sup> (LBSC+0.5 M SDC). The current density increased significantly at 800°C by 275%, from 154.10 mA.cm<sup>-2</sup> (pure LBSC) to 577.86 mA.cm<sup>-2</sup> (LBSC+0.5 M SDC). It is proven that the infiltration of 0.5 M SDC into the porous LBSC cathode significantly increases the current density value for the LBSC double perovskite cathodes, as shown in Table 1.

**Table 1.** The current density ( $i_o$ ) values of the LBSC and LBSC+0.5 M SDC cathodes were determined by the EIS method

Temperature (°C)	Current density ( $i_o$ )(mA.cm <sup>-2</sup> )	
	LBSC	LBSC+0.5 M SDC
600	11.13	19.19
650	25.17	38.99
700	72.28	83.84
750	88.15	314.82
800	154.10	577.86

The cathode microstructure is strongly related to electron and oxygen transport. These properties impact the performance of solid fuel cells (SOFC), including reaction kinetics, charge transport, and mass transport preprocess [30]. In general, the cathode layer in SOFC components is required to have homogeneous, dense, and highly porous grains. The highly porous cathode will facilitate oxygen transport to the active three-phase boundary (TPB) site. TPB is the interface area between the electrode, electrolyte, and fuel gas where the overall reaction occurs. The high ionic conductivity of SDC enlarges the active reaction zone, thereby decreasing resistance polarization ( $R_p$ ) and enhancing SOFC performance [31]. The microstructure of the LBSC|SDC|LBSC symmetric cell cross-section is shown in Figure 5.

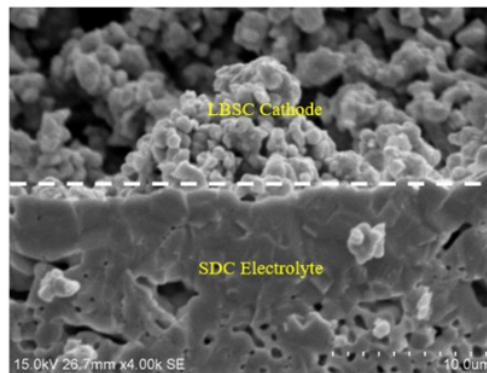


**Figure 5.** Symmetrical cross-section of cells observed using SEM

#### 4. Conclusion

This study focused on enhancing the performance of symmetrical cells by modifying the cathode surface. The current density value increased by 275% at 800°C. The activation energy ( $E_a$ ) of the polarization resistance of the LBSC+0.5 M SDC cathode was 47.9 kJ mol<sup>-1</sup>, which is 79.4% less than that of the LBSC sample without infiltration.  $E_a$  values of symmetrical cells LBSC+0.5 M SDC|SDC|LBSC+0.5 M SDC| in the order EIS > HF > LF. SDC nanoparticles actively amplify the electrochemical reaction between the layers of the electrode-electrolyte and the adsorption-desorption of oxygen diffusion between the layers of the cathode-gas surface, thereby significantly enhancing the performance of the symmetrical cell.

#### Acknowledgment

We thank Prof. Yen-Pei Fu for facilitating this research at the Department of Materials Science and Engineering, National Dong Hwa University, Taiwan.

#### References

- [1] Catarina Mendonça, António Ferreira, Diogo M. F. Santos, Towards the Commercialization of Solid Oxide Fuel Cells: Recent Advances in Materials and Integration Strategies, *Fuels*, 2, 4, (2021), 393–419 <https://doi.org/10.3390/fuels2040023>
- [2] Ruguang Ma, Gaoxin Lin, Yao Zhou, Qian Liu, Tao Zhang, Guangcun Shan, Minghui Yang, Jiacheng Wang, A review of oxygen reduction mechanisms for metal-free carbon-based electrocatalysts, *npj Computational Materials*, 5, 78, (2019), 1–15 <https://doi.org/10.1038/s41524-019-0210-3>
- [3] Xiao Xia Wang, Mark T. Swihart, Gang Wu, Achievements, challenges and perspectives on cathode catalysts in proton exchange membrane fuel cells for transportation, *Nature Catalysis*, 2, 7, (2019), 578–589 <https://doi.org/10.1038/s41929-019-0304-9>
- [4] Minghai Shen, Fujin Ai, Hailing Ma, Hui Xu, Yunyu Zhang, Progress and prospects of reversible solid oxide fuel cell materials, *iScience*, 24, 12, (2021), 103464 <https://doi.org/10.1016/j.isci.2021.103464>
- [5] Guangming Yang, Chao Su, Huangang Shi, Yinlong Zhu, Yufei Song, Wei Zhou, Zongping Shao, Toward reducing the operation temperature of solid oxide fuel cells: our past 15 years of efforts in cathode development, *Energy & Fuels*, 34, 12, (2020), 15169–15194 <https://doi.org/10.1021/acs.energyfuels.0c01887>
- [6] Kyeong Eun Song, Sung Hun Woo, Seung Wook Baek, Hyunil Kang, Won Seok Choi, Jun Young Park, Jung Hyun Kim, SmBa<sub>1-x</sub>Ca<sub>x</sub>Co<sub>2</sub>O<sub>5+d</sub> Layered Perovskite Cathodes for Intermediate Temperature-operating Solid Oxide Fuel Cells, *Frontiers in Chemistry*, 8, (2021), 628813 <https://doi.org/10.3389/fchem.2020.628813>
- [7] Xiaowei Liu, Fangjun Jin, Ning Sun, Jiangxin Li, Yu Shen, Fang Wang, Jinhua Li, Nd<sup>3+</sup>-deficiency double perovskite Nd<sub>1-x</sub>BaCo<sub>2</sub>O<sub>5,δ</sub> and performance optimization as cathode materials for intermediate-temperature solid oxide fuel cells, *Ceramics International*, 47, 23, (2021), 33886–33896 <https://doi.org/10.1016/j.ceramint.2021.08.301>
- [8] Sihyuk Choi, Seonyoung Yoo, Jiyoun Kim, Seonhye Park, Areum Jun, Sivaprakash Sengodan, Junyoung Kim, Jeeyoung Shin, Hu Young Jeong, YongMan Choi, Guntae Kim, Meilin Liu, Highly efficient and robust cathode materials for low-temperature solid oxide fuel cells: PrBa<sub>0.5</sub>Sr<sub>0.5</sub>Co<sub>2-x</sub>Fe<sub>x</sub>O<sub>5+δ</sub>, *Scientific Reports*, 3, 1, (2013), 1–6 <https://doi.org/10.1038/srep02426>
- [9] David Parfitt, Alexander Chroneos, Albert Tarancón, John A. Kilner, Oxygen ion diffusion in cation ordered/disordered GdBaCo<sub>2</sub>O<sub>5+δ</sub>, *Journal of Materials Chemistry*, 21, 7, (2011), 2183–2186 <https://doi.org/10.1039/C0JM02924F>
- [10] M. Jafari, H. Salamati, M. Zhiani, E. Shahsavari, Enhancement of an IT-SOFC cathode by introducing YSZ: Electrical and electrochemical properties of La<sub>0.6</sub>Ca<sub>0.4</sub>Fe<sub>0.8</sub>Ni<sub>0.2</sub>O<sub>3-δ</sub>-YSZ composites, *International Journal of Hydrogen Energy*, 44, 3, (2019), 1953–1966 <https://doi.org/10.1016/j.ijhydene.2018.10.151>
- [11] Mingfei Liu, Dong Ding, Kevin Blinn, Xiayi Li, Lifang Nie, Meilin Liu, Enhanced performance of LSCF cathode through surface modification, *International Journal of Hydrogen Energy*, 37, 10, (2012), 8613–8620 <https://doi.org/10.1016/j.ijhydene.2012.02.139>
- [12] Byoung Young Yoon, Joongmyeon Bae, Characteristics of nano La<sub>0.6</sub>Sr<sub>0.4</sub>Co<sub>0.2</sub>Fe<sub>0.8</sub>O<sub>3-δ</sub>-infiltrated La<sub>0.8</sub>Sr<sub>0.2</sub>Ga<sub>0.8</sub>Mg<sub>0.2</sub>O<sub>3-δ</sub> scaffold cathode for enhanced oxygen reduction, *International Journal of Hydrogen Energy*, 38, 30, (2013), 13399–13407 <https://doi.org/10.1016/j.ijhydene.2013.07.087>
- [13] Dong Ding, Xiayi Li, Samson Yuxiu Lai, Kirk Gerdes, Meilin Liu, Enhancing SOFC cathode performance by surface modification through infiltration, *Energy & Environmental Science*, 7, 2, (2014), 552–575 <https://doi.org/10.1039/C3EE42926A>
- [14] Ye Lin, Chao Su, Cheng Huang, Ju Sik Kim, Chan Kwak, Zongping Shao, A new symmetric solid oxide fuel cell with a samaria-doped ceria framework and a silver-infiltrated electrocatalyst, *Journal of Power Sources*, 197, (2012), 57–64 <https://doi.org/10.1016/j.jpowsour.2011.09.040>
- [15] Feng Su, Yanxiang Zhang, Meng Ni, Changrong Xia, Sm<sub>0.5</sub>Sr<sub>0.5</sub>CoO<sub>3</sub>-Ce<sub>1.8</sub>Sm<sub>0.2</sub>O<sub>1.9</sub> electrodes enhanced by Sm<sub>0.5</sub>Sr<sub>0.5</sub>CoO<sub>3</sub> impregnation for proton conductor based solid oxide fuel cells, *International Journal of Hydrogen Energy*, 39, 6, (2014), 2685–2691 <https://doi.org/10.1016/j.ijhydene.2013.12.012>
- [16] Jian Shen, Yubo Chen, Guangming Yang, Wei Zhou, Moses O. Tadé, Zongping Shao, Impregnated LaCo<sub>0.3</sub>Fe<sub>0.67</sub>Pd<sub>0.03</sub>O<sub>3-δ</sub> as a promising electrocatalyst for “symmetrical” intermediate-temperature solid oxide fuel cells, *Journal of Power Sources*, 306, (2016), 92–99 <https://doi.org/10.1016/j.jpowsour.2015.12.021>
- [17] San Ping Jiang, Nanoscale and nano-structured electrodes of solid oxide fuel cells by infiltration: advances and challenges, *International Journal of Hydrogen Energy*, 37, 1, (2012), 449–470 <https://doi.org/10.1016/j.ijhydene.2011.09.067>
- [18] Yen-Pei Fu, Jie Ouyang, Chien-Hung Li, Shao-Hua Hu, Characterization of nanosized Ce<sub>0.8</sub>Sm<sub>0.2</sub>O<sub>1.9</sub>-infiltrated Sm<sub>0.5</sub>Sr<sub>0.5</sub>Co<sub>0.8</sub>Cu<sub>0.2</sub>O<sub>3-δ</sub> cathodes for solid oxide fuel cells, *International Journal of Hydrogen*

- Energy*, 37, 24, (2012), 19027–19035  
<https://doi.org/10.1016/j.ijhydene.2012.09.012>
- [19] Fucun Wang, Dengjie Chen, Zongping Shao,  $\text{Sm}_{0.5}\text{Sr}_{0.5}\text{CoO}_{3-\delta}$ -infiltrated cathodes for solid oxide fuel cells with improved oxygen reduction activity and stability, *Journal of Power Sources*, 216, (2012), 208–215  
<https://doi.org/10.1016/j.jpowsour.2012.05.068>
- [20] Lifang Nie, Mingfei Liu, Yujun Zhang, Meilin Liu,  $\text{La}_{0.6}\text{Sr}_{0.4}\text{Co}_{0.2}\text{Fe}_{0.8}\text{O}_{3-\delta}$  cathodes infiltrated with samarium-doped cerium oxide for solid oxide fuel cells, *Journal of Power Sources*, 195, 15, (2010), 4704–4708  
<https://doi.org/10.1016/j.jpowsour.2010.02.049>
- [21] Adi Subardi, Yen-Pei Fu, Electrochemical and thermal properties of  $\text{SmBa}_{0.5}\text{Sr}_{0.5}\text{Co}_2\text{O}_{5+\delta}$  cathode impregnated with  $\text{Ce}_{0.8}\text{Sm}_{0.2}\text{O}_{1.9}$  nanoparticles for intermediate-temperature solid oxide fuel cells, *International Journal of Hydrogen Energy*, 42, 38, (2017), 24338–24346  
<https://doi.org/10.1016/j.ijhydene.2017.08.010>
- [22] Adi Subardi, Meng-Hsien Cheng, Yen-Pei Fu, Chemical bulk diffusion and electrochemical properties of  $\text{SmBa}_{0.6}\text{Sr}_{0.4}\text{Co}_2\text{O}_{5+\delta}$  cathode for intermediate solid oxide fuel cells, *International Journal of Hydrogen Energy*, 39, 35, (2014), 20783–20790  
<https://doi.org/10.1016/j.ijhydene.2014.06.134>
- [23] Yen - Pei Fu, Shaw - Bing Wen, Chi - Hua Lu, Preparation and characterization of samaria - doped ceria electrolyte materials for solid oxide fuel cells, *Journal of the American Ceramic Society*, 91, 1, (2008), 127–131  
<https://doi.org/10.1111/j.1551-2916.2007.01923.x>
- [24] Adi Subardi, Ching-Cheng Chen, Yen-Pei Fu, Oxygen transportation, electrical conductivity and electrochemical properties of layered perovskite  $\text{SmBa}_{0.5}\text{Sr}_{0.5}\text{Co}_2\text{O}_{5+\delta}$ , *International Journal of Hydrogen Energy*, 42, 8, (2017), 5284–5294  
<https://doi.org/10.1016/j.ijhydene.2016.11.123>
- [25] Kanghee Jo, Jooyeon Ha, Jiseung Ryu, Eunkyung Lee, Heesoo Lee, DC 4-Point Measurement for Total Electrical Conductivity of SOFC Cathode Material, *Applied Sciences*, 11, 11, (2021), 4963  
<https://doi.org/10.3390/app11114963>
- [26] Abhishek Jaiswal, Eric D. Wachsman, Bismuth-ruthenate-based cathodes for IT-SOFCs, *Journal of The Electrochemical Society*, 152, 4, (2005), A787  
<https://doi.org/10.1149/1.1866093>
- [27] Fuchang Meng, Tian Xia, Jingping Wang, Zhan Shi, Jie Lian, Hui Zhao, Jean-Marc Bassat, Jean-Claude Grenier, Evaluation of layered perovskites  $\text{YBa}_{1-x}\text{Sr}_x\text{Co}_2\text{O}_{5+\delta}$  as cathodes for intermediate-temperature solid oxide fuel cells, *International Journal of Hydrogen Energy*, 39, 9, (2014), 4531–4543  
<https://doi.org/10.1016/j.ijhydene.2014.01.008>
- [28] Jiyou Kim, Won-yong Seo, Jeeyoung Shin, Meilin Liu, Guntae Kim, Composite cathodes composed of  $\text{NdBa}_{0.5}\text{Sr}_{0.5}\text{Co}_2\text{O}_{5+\delta}$  and  $\text{Ce}_{0.9}\text{Gd}_{0.1}\text{O}_{1.95}$  for intermediate-temperature solid oxide fuel cells, *Journal of Materials Chemistry A*, 1, 3, (2012), 515–519  
<https://doi.org/10.1039/C2TA00025C>
- [29] Stuart B. Adler, Factors governing oxygen reduction in solid oxide fuel cell cathodes, *Chemical Reviews*, 104, 10, (2004), 4791–4844  
<https://doi.org/10.1021/cr020724o>
- [30] Jin Hyun Nam, Dong Hyup Jeon, A comprehensive micro-scale model for transport and reaction in intermediate temperature solid oxide fuel cells, *Electrochimica Acta*, 51, 17, (2006), 3446–3460  
<https://doi.org/10.1016/j.electacta.2005.09.041>
- [31] Shengli Pang, Xuening Jiang, Xiangnan Li, Qian Wang, Zhixian Su, Characterization of Ba-deficient  $\text{PrBa}_{1-x}\text{Co}_2\text{O}_{5+\delta}$  as cathode material for intermediate temperature solid oxide fuel cells, *Journal of Power Sources*, 204, (2012), 53–59  
<https://doi.org/10.1016/j.jpowsour.2012.01.034>

# Effect of Infiltration Ce<sub>0.8</sub>Sm<sub>0.2</sub>O<sub>1.9</sub> Against Double Perovskite Performance LaBa<sub>0.5</sub>Sr<sub>0.5</sub>Co<sub>2</sub>O<sub>5+δ</sub> as IT-SOFC Cathode

---

## ORIGINALITY REPORT

---

13%

SIMILARITY INDEX

7%

INTERNET SOURCES

12%

PUBLICATIONS

2%

STUDENT PAPERS

---

## MATCH ALL SOURCES (ONLY SELECTED SOURCE PRINTED)

---

1%

★ Pingping Wu, Yanting Tian, Zhe Lü, Xu Zhang, Lili Ding. "Electrochemical performance of La<sub>0.65</sub>Sr<sub>0.35</sub>MnO<sub>3</sub> oxygen electrode with alternately infiltrated Sm<sub>0.5</sub>Sr<sub>0.5</sub>CoO<sub>3-δ</sub> and Sm<sub>0.2</sub>Ce<sub>0.8</sub>O<sub>1.9</sub> nanoparticles for reversible solid oxide cells", International Journal of Hydrogen Energy, 2021

Publication

---

Exclude quotes Off

Exclude matches Off

Exclude bibliography On



# Effect of Infiltration Ce<sub>0.8</sub>Sm<sub>0.2</sub>O<sub>1.9</sub> Against Double Perovskite Performance LaBa<sub>0.5</sub>Sr<sub>0.5</sub>Co<sub>2</sub>O<sub>5+δ</sub> as IT-SOFC Cathode

---

GRADEMARK REPORT

---

FINAL GRADE

**/0**

GENERAL COMMENTS

**Instructor**

---

PAGE 1

---

PAGE 2

---

PAGE 3

---

PAGE 4

---

PAGE 5

---

PAGE 6

---